CFD ANALYSIS OF THE PULVERIZED COAL COMBUSTION PROCESS IN A BOILER OF A THERMAL POWER PLANT: INFLUENCE OF TILTED INLET FLOW OF FUEL AND AIR ON THE NO_x FORMATION

Cristiano V. da Silva, cristiano@uticer.edu.br
Universidade Regional Integrada do Alto Uruguai e das Missões – URI. Av. Sete de Setembro, 1621, Erechim, RS, Brasil.

Arthur B. Beskow, arthurbb@pucrs.br
Maria L. S. Indrusiak, sperbindrusiak@via-rs.net
José W. M. Kaehler, kaehlerj@pucrs.br
Pontifícia Universidade Católica do Rio Grande do Sul – PUCRS. Av. Ipiranga, n.6681, 90619-900, Porto Alegre – RS – Brasil

Abstract. *The strategic role of energy and the current concerning with greenhouse effects, energetic and exergetic efficiency of fossil fuel combustion greatly enhance the importance of the studies of complex physical and chemical processes occurring inside boilers of thermal power plants. The state of the art in computational fluid dynamics and the availability of commercial codes encourage numeric studies of the combustion processes. In the present work the commercial software CFX©Ansys Europe Ltd. has been used to study the influence of tilted inlet flow of fuel and air on the NO_x formation in a boiler of a 160 MW thermal power plant. The behavior of the air and pulverized coal flows through the burners was analyzed and the three-dimensional flue (or exhaust) gas flow through combustion chamber and heat exchangers was reproduced in the numeric simulation. It was verified that the tilt of the burners have a significant effect on the NO_x formation.*

Keywords*: Combustion, Computational Fluid Dynamic, Thermal Power Plant, NO_x formation.*

1. INTRODUCTION

In some parts of the world coal is an important energy resource for meeting the future demand for electricity, as coal reserves are much greater than those of other fossil fuels. However, the efficiency and clean utilization of this fuel is a major problem in combustion processes. In recent years, the interest on performance optimization of large utility boilers has become very relevant, aiming at extending their lifetime, increasing the thermal efficiency and reducing the pollutant emissions, particularly the NO_x emissions.

Coal reserves in Brazil, which are used mainly for electricity production in large utility boilers, are enough to meet the next 200 years demand. Nonetheless, in order to face the competition from renewable, natural gas and nuclear energy sources, some main problems must be solved, as to reduce CO_2 emissions through increasing efficiency (Williams et al., 2000). Also NO_x and SO_x emissions should be reduced to environmentally acceptable levels. An efficient operation of combustion chambers of these boilers depends on the proper knowledge of the oxidation reactions and heat transfer between the combustion products and the chamber walls and heat exchangers, which requires a detailed analysis of the governing mechanisms. A number of combustion modeling methodologies is now available, but only a few are able to account the process in its entirety. Eaton et al. (1999) present a revision of combustion models. The models are generally based on the fundamental conservation equations of mass, energy, chemical species and momentum, while the problem closure is achieved by turbulence models such as the $k-\varepsilon$ (Launder and Sharma, 1974), combustion models like Arrhenius (Kuo, 1996, Turns, 2000), Magnussen - EBU - "Eddy Breakup" (Magnussen and Hjertager, 1976), radiative transfer models based on the Radiative Transfer Equation - RTE (Carvalho et al., 1991) and models to devolatilisation and combustion of solid and liquid fuels.

Abbas et al. (1993) describe an experimental and predicted assessment of the influence of coal particle size on the formation of NO_x of a swirl-stabilized burner in a large-scale laboratory furnace. Three particle size distributions, 25, 46, and 121 μm average size, of high volatile coal were fired under the same operation conditions. The data presented combine detailed in-flame measurements of gas temperature, gas species concentrations of CO, CH_4, O_2, NO, HCL, NH_3, particle burnout, and "on-line" N_2O, with the complementary predicted studies. The supporting predicted results are in good agreement with experimental data. Although the NO emission trends with particle size are similar, predicted values for each fraction are higher, suggesting a limitation in the NO reducing mechanisms used in the model. Three mechanisms – thermal, fuel and prompt - were used to calculate the NO_x formation.

Xu et al. (2000) employed the CFD code to solve a coal combustion process in a front wall pulverized coal fired utility boiler of 350 MWe with 24 swirl burners installed at the furnace front wall. Five different cases with 100, 95, 85, 70 and 50% boiler full load were simulated. Comparisons were addressed, with good agreement between predicted and measured results in the boiler for all but one cases thus validating the models and the algorithm employed in the computation.

Li et al. (2003) numerically investigated the combustion process using a pure two-fluid model (instead of the Eulerian gas - Lagrangian particle models) for simulating tree-dimensional turbulent reactive flows and coal combustion. To improve the simulation of the flow field and NO_x formation, a modified $K-\varepsilon-k_p$ two-phase

turbulence model and a second-order-moment (SOM) reactive rate model are proposed. The proposed models are used to simulate NO formation of methane-air combustion, and the prediction results are compared with those using the pure presumed-PDF (Probability Density Function)-finite-reaction-rate model and experimental data. The proposed models are also used to predict the coal combustion and NO_x formation at the exit of a double air register swirl pulverized-coal burner. The predicted results indicate that a pulverized-coal concentrator installed in the primary-air tube of burner has a strong effect on the coal combustion and NO_x formation.

In a numerical investigation, Kurose et al. (2004) employed a tree-dimensional simulation to the pulverized coal combustion field in a furnace equipped whit a low-NO_x burner, called CI-α, to investigate in details the combustion processes. The validities of existing NO_x formation and reduction models were investigated too. The results show that a recirculation flow is formed in high-gas-temperature region near the CI-α burner outlet, and this lengthens the residence time of coal particles in this high-gas-temperature region, promotes the evolution of volatile matter and the process of char reaction, and produces an extremely low-O_2 region for effective NO reduction.

Zhang et al. (2005) present a numerical investigation on the coal combustion process using an algebraic unified second-order moment (AUSM) turbulence-chemistry model to calculate the effect of particle temperature fluctuation on char combustion. The AUSM model was used to simulate gas-particles flows, in coal combustion including the sub-models as the $k-\varepsilon-k_p$ two-phase turbulence model, the EBU-Arrhenius volatile and CO combustion model, and the six-flux radiation model. The simulation results indicate that, the AUSM char combustion model is far preferable to the old char combustion model, since the later totally eliminates the influence of particle temperature fluctuation on char combustion rate.

Bosoaga et al. (2006) presents a study developing a CFD model for the combustion of low-grade lignite and to characterize the combustion process in the test furnace, including the influence of the geometry of burner and furnace. A number of computations were made in order to predict the effect of coal particle size, the moisture content of lignite, and the influence of combustion temperature and operation of the support methane flame on the furnace performance and emissions. The influence of pre-drying of lignite was also modeled to investigate the effects of reduced fuel consumption and CO_2 emissions. It was founded that the increasing of moisture tends to reduce NO_x, and the methane support flame greatly increased NO_x and under the conditions used almost by a factor of three.

In another work, Backreedy et al. (2006) present a numerical and experimental investigation on the coal combustion process to predict the combustion process of pulverized coal in a test furnace of 1 MW thermal. The furnace used also contains a triple-staged low-NO_x swirl burner. A number of simulations were made using a number of coals in order to calculate NO_x and the unburned carbon-in-ash, the later being a sensitive test for the accuracy of the char combustion model. The NO_x incorporates fuel-NO, thermal, and prompt mechanisms to predict the NO formation on the combustion processes.

This research work presents a numeric simulation approach, using a commercial CFD code. The subject of the study is the boiler of a 160 MW unit of a thermal power plant commercially operated by CGTEE in Candiota-RS, in the core of the Brazilian coal reserves region. The goal of this work is to investigate the effect of the tilt of the burners on the combustion process and NO_x formation. The case studied was a -15º displacement (descendent jets) on the injection of fuel and air relative to the horizontal plane, the results being compared to the original project case (horizontal jets).

2. MATHEMATICAL FORMULATION

The proposed task can be stated as follows: considering steady combustion of raw coal in air, for a boiler combustion chamber, compute the temperature, chemical species concentrations and the velocity fields for multi component flow (gas mixture and raw coal particles), and verify the influence of the operation parameters, such as heterogeneous condition for fuel and air flow in the chamber, on the combustion process and NO_x formation.

The complete chemical reaction of the raw coal used at this work, including two devolatilisation processes, is modeled according to the basic scheme showed in Fig. 1.

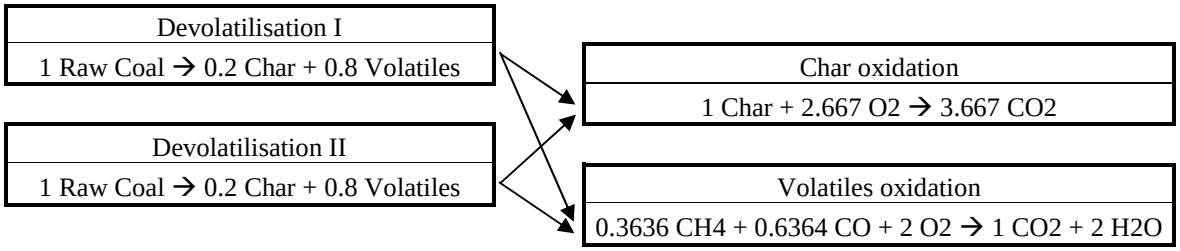

Figure 1 - Basic scheme of the full chemical reactions of the raw coal.

As basic assumptions, it is considered that the mass fractions of volatiles are 0.3636 of methane and 0.6364 of carbon monoxide, and that the combustion processes of these volatiles occur at finite rates. The methane oxidation is modeled by two global steps, given by:

$$2CH_4^{(16)} + 3\left(O_2^{(32)} + 3.76N_2^{(28)}\right) \rightarrow 2CO^{(28)} + 4H_2O^{(18)} + 11.28N_2^{(28)} \quad (1)$$

$$2CO^{(28)} + 1\left(O_2^{(32)} + 3.76N_2^{(28)}\right) \rightarrow 2CO_2^{(28)} + 3.76N_2^{(28)} \quad (2)$$

Equation 2 also models the combustion of carbon monoxide resulting from the devolatilisation processes. The formation of NO_x is modeled by Zeldovich's mechanisms using two different ways, the thermal-NO and the Prompt-NO, where the first, that is predominant at temperatures above 1800K, is given by tree-step chemical reaction mechanisms:

$$O^{(16)} + N_2^{(28)} \rightarrow NO^{(30)} + N^{(14)} \quad (3)$$

$$N^{(14)} + O_2^{(32)} \rightarrow NO^{(30)} + O^{(16)} \quad (4)$$

In sub or near stoichiometric conditions, a third reaction is also used

$$OH^{(17)} + N^{(14)} \rightarrow NO^{(30)} + H^{(1)} \quad (5)$$

where the chemical reaction rates are predicted by Arrhenius equation.

For the prompt-NO, formed at temperatures lower than 1800 K, where radicals can react with molecular nitrogen to form HCN, which may be oxidized to NO under flame conditions. The complete mechanism is not straightforward. However, De Soete proposed a single reaction rate to describe the NO source by Fennimore mechanism, which is used at this work. Arrhenius equations are used for predict this chemical reaction rate.

For multicomponent fluid, scalar transport equations are solved for velocity, pressure, temperature and chemical species. Additional equations are solved to determine how the components of the fluid are transported within the fluid. The bulk motion of the fluid is modeled using single velocity, pressure, temperature, chemical species and turbulence fields.

2.1. Mass and species conservation

Each component has its own Reynolds-averaged equation for mass conservation, which, considering incompressible and stationary flow can be written in tensor notation as:

$$\frac{\partial\left(\tilde{\rho}_i \tilde{U}_j\right)}{\partial x_j} = \frac{\partial}{\partial x_j}\left(\rho_i\left(\tilde{U}_{ij} - \tilde{U}_j\right) - \overline{\rho_i "U_j"}\right) + S_i \quad (6)$$

where $\tilde{U}_j = \sum\left(\tilde{\rho}_i \tilde{U}_{ij}\right)\Big/\overline{\rho}$. $\tilde{\rho}_i$ and $\overline{\rho}$ are the mass-average density of fluid component i in the mixture and average density, respectively, x is the spatial coordinate, $\tilde{U}$ is the vector of velocity and $\tilde{U}_{ij}$ is the mass-averaged velocity of fluid component i. The term $\rho_i\left(\tilde{U}_{ij} - \tilde{U}_j\right)$ represents the relative mass flow, and S_i is the source term for component i which includes the effects of chemical reactions. Note that if all the equations represented by Eq. (6) are summed over all components, and the source term is set to zero, the result is the standard continuity equation.

The relative mass flow term accounts for differential motion of the individual components. At this work, this term is modeled for the relative motion of the mixture components and the primary effect is that of concentration gradient. Therefore,

$$\rho_i\left(\tilde{U}_{ij} - \tilde{U}_j\right) = \frac{\rho D_i}{\overline{\rho}} \frac{\partial \tilde{\rho}_i}{\partial x_i} \quad (7)$$

where D_i is the kinematic diffusivity. The mass fraction of component i is defined as $\tilde{Y}_i = \tilde{\rho}_i \big/ \overline{\rho}$. Substituting this expressions into Eq. (7) and modeling the turbulent scalar flows using the eddy dissipation assumption it follows that

$$\frac{\partial}{\partial x_j}\left(\overline{\rho}\tilde{U}_j \tilde{Y}_i\right) = \frac{\partial}{\partial x_j}\left(\left(\rho D_i + \frac{\mu_t}{Sc_t}\right)\frac{\partial \tilde{Y}_i}{\partial x_j}\right) + S_i \quad (8)$$

where μ_t is the turbulent viscosity and Sc_t is the turbulent Schmidt number. Note that the sum of component mass fractions over all components is equal to one.

2.2. Momentum conservation

For the fluid flow the momentum conservation equations are given by:

$$\frac{\partial}{\partial x_j}\left(\overline{\rho}\tilde{U}_i\tilde{U}_j\right) = -\frac{\partial p^*}{\partial x_j}\delta + \frac{\partial}{\partial x_j}\left(\mu_{eff}\frac{\partial \tilde{U}_i}{\partial x_j}\right) + \frac{\partial \tilde{U}}{\partial x_j \partial x_i} + S_U \tag{9}$$

where $\mu_{eff} = \mu + \mu_t$ and μ is the mixture dynamic viscosity and μ_t is the turbulent viscosity, defined as $\mu_t = C_\mu \rho\, k^2/\varepsilon$. The term $p^* = \overline{p} - (2/3)k$ is the modified pressure, C_μ is an empirical constant of the turbulence model, $\overline{p}$ is the time-averaged pressure of the gaseous mixture, and δ is the Krönecker delta function. S_U is the source term, introduced to model the buoyancy and drag force due to the transportation particles, and other mathematical terms due to turbulence models. The Boussinesq model is used to represent the buoyancy force due to density variations.

2.3. The $k-\varpi$ turbulence model

The equations for turbulent kinetic energy, k, and its turbulent frequency, ϖ, are:

$$\frac{\partial}{\partial x_j}\left(\tilde{\rho}\tilde{U}_j k\right) = \left(\frac{\partial}{\partial x_j}\left(\mu + \frac{\mu_t}{\sigma_k}\right)\frac{\partial k}{\partial x_j}\right) + P_k - \beta'\rho k\varpi \tag{10}$$

$$\frac{\partial}{\partial x_j}\left(\tilde{\rho}\tilde{U}_j \varpi\right) = \left(\frac{\partial}{\partial x_j}\left(\mu + \frac{\mu_t}{\sigma_\varpi}\right)\frac{\partial \varpi}{\partial x_j}\right) + \alpha\frac{\varpi}{k}P_k - \beta\rho\varpi^2 \tag{11}$$

where β', β and α are empirical constants of the turbulence model, σ_k and σ_ϖ are the Prandtl numbers of the kinetic energy and frequency, respectively, and P_k is the term who accounts for the production or destruction of the turbulent kinetic energy.

$$P_k = \mu_t\left(\frac{\partial U_i}{\partial x_j} + \frac{\partial U_j}{\partial x_i}\right) \tag{12}$$

2.4. Energy conservation

Considering the transport of energy due to the diffusion of each chemical species, the energy equation can be written as

$$\frac{\partial}{\partial x_j}\left(\overline{\rho}\tilde{U}_j\tilde{h}\right) = \frac{\partial}{\partial x_j}\left(\left(\mu + \frac{\mu_t}{\sigma_\varpi}\right)\frac{\partial \tilde{h}}{\partial x_j} + \sum_i^{Nc}\overline{\rho}D_i\tilde{h}_i\frac{\partial \tilde{Y}_i}{\partial x_j} + \frac{\mu_t}{\mathrm{Pr}_t}\frac{\partial \tilde{h}}{\partial x_j}\right) + S_{rad} + S_{rea} \tag{13}$$

where $\tilde{h}$ and c_p are the average enthalpy and specific heat of the mixture. The latter is given by

$$c_p = \sum_\alpha \tilde{Y}_\alpha c_{p,\alpha} \tag{14}$$

where $c_{p,\alpha}$ and $\tilde{Y}$ are the specific heat and the average mass fraction of the α-th chemical species, κ is the thermal conductivity of the mixture, Pr_t is the turbulent Prandtl number, and S_{rad} and S_{rea} represent the sources of thermal energy due to the radiative transfer and to the chemical reactions. The term S_{rea} can be written as:

$$S_{rea} = \sum_\alpha\left[\frac{h_\alpha^0}{\overline{MM}_\alpha} + \int_{\tilde{T}_{ref,\alpha}}^{\tilde{T}} c_{p,\alpha}\, d\tilde{T}\right]\overline{R_\alpha} \tag{15}$$

where $\tilde{T}$ is the average temperature of the mixture, h_α^0 and $\tilde{T}_{ref,\alpha}$ are the formation enthalpy and the reference temperature of the α-th chemical species. To complete the model, the density of mixture can be obtained from the ideal

gas state equation (Kuo, 1996; Fluent, 1997; Turns, 2000), $\overline{\rho} = p\overline{MM}\left(\overline{R}\,\tilde{T}\right)^{-1}$, where p is the combustion chamber operational pressure, which is here set equal to 1 atm (Spalding, 1979), and $\overline{MM}$ is the mixture molecular mass. The aforementioned equations are valid only in the turbulent core, where $\mu_t >> \mu$. Close to the wall, the logarithmic law of the wall is used (Launder and Sharma, 1974).

To consider thermal radiation exchanges inside the combustion chamber, the Discrete Transfer Radiation Model - DTRM is employed (Carvalho et al., 1991), considering that the scattering is isotropic. The effect of the wavelength dependence is not considered, and the gas absorption coefficient is considered uniform inside the combustion chamber and its value is 0.5 m^{-1}. Then, the Radiative Transfer Equation – RTE is integrated within its spectral band and a modified RTE can be written as

$$\frac{dI(r,s)}{dS} = \frac{K_a \sigma \tilde{T}^4}{\pi} - K_a I(r,s) + S'' \tag{16}$$

At the equations above, σ is the Stefan-Boltzmann constant (5.672 x 10^{-8} W/m^2K^4), r is the vector position, s is the vector direction, S is the path length, K_a is the absorption coefficient, I is the total radiation intensity which depends on position and direction, and S'' is the radiation source term, where one can be computed the radiation emission of the particles. The radiative properties required for an entrained particle phase are the absorption coefficients and scattering phase function, which depend on the particle concentration, size distribution, and effective complex refractive indices. However, optical properties of coal are not well characterized (Eaton et al., 1999). Generally, as a starting point to arrive at a tractable method for calculating radiative properties, the particles are assumed to be spherical and homogeneous. At this work, the heat transfer from gas mixture to particle considers that the particles are opaque bodies whit emissivity equal to one, and the Hanz-Marshall's correlation is used to model the heat transfer coupling between the gas mixture flow and the particles.

2.5. The E-A (Eddy Breakup – Arrhenius) chemical reactions model

The reduced chemical reactions model that is employed here assumes finite rate reactions and a steady state turbulent process to volatiles combustion. In addition, it is considered that the combined pre-mixed and non-premixed oxidation occurs in two global chemical reaction steps, and involving only six species: oxygen, methane, nitrogen, water vapor, carbon dioxide and carbon monoxide. A conservation equation is required for each species, with the exception of nitrogen. Thus, one has the conservation equation for the α-th chemical species, given by Eq. (8), where the source term, S_i, considers the average volumetric rate of formation or destruction of the α-th chemical species at all chemical reactions. This term is computed from the summation of the volumetric rates of formation or destruction in all the k-th equations where the α-th species is present, $\overline{R_{\alpha,k}}$. Thus, $\overline{R_\alpha} = \sum_k \overline{R_{\alpha,k}}$.

The rate of formation or destruction, $\overline{R_{\alpha,k}}$, can be obtained from an Arrhenius kinetic rate relation, which takes into account the turbulence effect, such as Magnussen's equations (Eddy Breakup) (Magnussen and Hjertager, 1976), or a combination of the two formulations, the so called Arrhenius-Magnussen's model (Eaton et al., 1999; CFX Inc., 2004). Such relations are appropriate for a wide range of applications, for instance, laminar or turbulent chemical reactions with or without pre-mixing. The Arrhenius equation can be written as follows:

$$\overline{R_{\alpha,k,Chemical}} = -\eta_{\alpha,k}\overline{MM}_\alpha \tilde{T}^{\beta_k} A_k \Pi_\alpha \tilde{C}_\alpha^{\gamma_{\alpha,k}} \exp\left(\frac{-E_k}{\overline{R}\,\tilde{T}}\right) \tag{17}$$

where β_k is the temperature exponent in each chemical reaction k, which is obtained empirically together with the energy activation E_k and the coefficient A_k. Π_α is the product symbol, $\tilde{C}_\alpha$ is the molar concentration of the α-th chemical species, $\gamma_{\alpha,k}$ is the concentration exponent in each reaction k, $\overline{R}$ is the gas constant, $\overline{MM}_\alpha$ and $\eta_{\alpha,k}$ are the molecular mass and the stoichiometric coefficient of α in the k-th chemical reaction.

In the Eddy-Breakup or Magnussen's model, the chemical reaction rates are based on the theories of vortex dissipation in the presence of turbulence. Thus, for diffusive flames:

$$\overline{R_{\alpha,k,EBU}} = -\eta_{\alpha,k}\overline{MM}_\alpha A \overline{\rho}\frac{\varepsilon}{k}\frac{\tilde{Y}_{\alpha^*}}{\eta_{\alpha^*,k}\overline{MM}_{\alpha^*}} \tag{18}$$

where the index α^* represents the reactant α that has the least value of $\overline{R_{\alpha,k,EBU}}$.

In the presence of premixing, a third relation for the Eddy Breakup model is necessary, so that

$$\overline{R_{\alpha,k,\mathrm{Premixing}}} = \eta_{\alpha,k}\,\overline{MM}_{\alpha} AB\bar{\rho}\frac{\varepsilon}{k}\frac{\sum_{p}\tilde{Y}_{p}}{\sum_{p}\eta_{p,k}\overline{MM}_{p}} \tag{19}$$

where the index p represents the gaseous products of the combustion. A and B are empirical constants that are set as 4 and 0.5 (Magnussen and Hjertager, 1976). Magnussen's model, Eqs. (18) and (19), can be applied to both diffusive and pre-mixed flames, or for the situation where both flames coexist, taking the smallest rate of chemical reaction.

Finally, for the Arrhenius-Magnussen model, given by Eqs. (17), (18) and (19), the rate of formation or destruction of the chemical species is taken as the least one between the values obtained from each model. It follows that

$$\overline{R_{\alpha,k}} = \min\left(\overline{R_{\alpha,k,Chemical}}, \overline{R_{\alpha,k,EBU}}, \overline{R_{\alpha,k,\mathrm{Premixed}}}\right) \tag{20}$$

2.6 The coal decomposition

Pulverized coal particles are treated at this work as non-interacting spheres with internal reactions and heat transfer and full coupling of mass, momentum and energy with the gaseous phase. The combustion of coal particles is a two stage process: the devolatilisation of raw coal particle followed by oxidation of residual char to leave incombustible ash. The devolatilisation was modeled with two competing reactions (see Fig. 1) in order to deal with the strong dependence on temperature and heating rate of the bituminous coal. The two equations have different rate parameters and volatile yields. The yield fractions for the lower temperature equation were obtained from proximate analysis and to the ones for the higher temperature equation were given the values suggested by Li et al. (2003). The model adopted for the char burn out computes the rate of the reaction taking into account the rate of diffusion of oxygen within the pores of the char particle and its partial pressure at the particle surface (Kanury, 1975). Particle size plays an important role in the char combustion process and is usually modeled by a statistical distribution like the one developed by Rosin-Rammler (Brown, 1995), with the parameters adjusted from pulverized coal analysis.

2.6.1 The coal devolatilisation model

The devolatilisation of the coal is modeled using the generic Arrhenius reactions capability in two steps (Ubhayakar et al., 1976) in which two reactions with different rate parameters and volatiles yields compete to pyrolyse the raw coal. The first reaction dominates at lower particle temperatures and has a yield Y_1 lower than the yield Y_2 of the second reaction which dominates at higher temperatures. As a result, the final yields of volatiles will depend on the temperature history of the particle, and will increase with temperature, lying somewhere between Y_1 and Y_2. In this model, the mass fraction of the raw coal is specified as the mass fraction of volatiles (here methane and carbon monoxide, see Fig. 1) since all this material could be converted to volatiles.

At time t, it is assumed that a coal particle consist of mass of raw coal (C_O), mass of residual char (C_{ch}) after devolatilisation has occurred, and mass of ash (A). The rate constants k_1 and k_2 of two reactions determine the rate of conversion of the raw coal:

$$\frac{dC_O}{dt} = -(k_1 + k_2)C_O \tag{21}$$

the rate of volatiles production is given by

$$\frac{dV}{dt} = (Y_1 k_1 + Y_2 k_2)C_O \tag{22}$$

and so the rate of char formation is

$$\frac{dC_{ch}}{dt} = ((1-Y_1)k_1 + (1-Y_2)k_2)C_O \tag{23}$$

2.6.2 The Field Char Oxidation model

The oxygen diffusion rate is given by $k_d(p_g - p_S)$, where p_g is the partial pressure of oxygen in the furnace gases far from particle boundary layer and p_S is the oxygen pressure at the particle surface. The value of k_d is given by $k_d = D_{ref} R_p^{-1}\left(T_p - \tilde{T}_g\left(2T_{ref}\right)^{-1}\right)^{\alpha} p_A/p$, where R_p is the particle radius, T_p is the particle temperature, $\tilde{T}_g$ is the far-field

gas temperature, p_A is atmospheric pressure, D_{ref} is the dynamic diffusivity, and α is the exponent with value 0.75. The char oxidation rate per unit area of particle surface is given by $k_c p_s$. The chemical rate coefficient is given by, $k_c = A_c \exp(-T_c/T_p)$, where the parameters A_c and T_c depends on the type of coal. The overall char reaction rate of a particle is given by $\left(k_d^{-1} + k_c^{-1}\right)^{-1} C_{O_2} 4\pi R_p^2 \overline{p}/p_A$, and is controlled by the smallest of the two rates, k_d and k_c.

3. BOILER DESCRIPTION

The boiler under consideration is part of a pulverized coal (PC) power plant operating in a subcritical steam cycle. The tangential firing combustion chamber is rectangular in shape with four burners firing from each corner, forming a large vortex in the center of the chamber. The evaporation process occurs mainly in the tubes covering the boiler walls. In the upper middle of the boiler are the reheater (LTR, HTR), superheater (LTS, HTS) and economizer (ECO2) tube banks. The second stage of the boiler comprises a large rectangular curved duct, the first economizer (ECO1) tube bank and the regenerative air heater (Ljungström). From there the flue gases are directed through the electrostatic precipitator to the chimney. Figure 2-a shows the general disposition of the boiler heat exchangers and burners.

The primary and secondary air paths are also shown, departing from the fans (PAF, SAF) through the air heater and coal silos (only for the primary air) to the burners. The burner disposition at the corners is shown at Fig 2-b. They are aligned with the diagonal lines with a horizontal angular displacement in order to create a vortex in the flow.

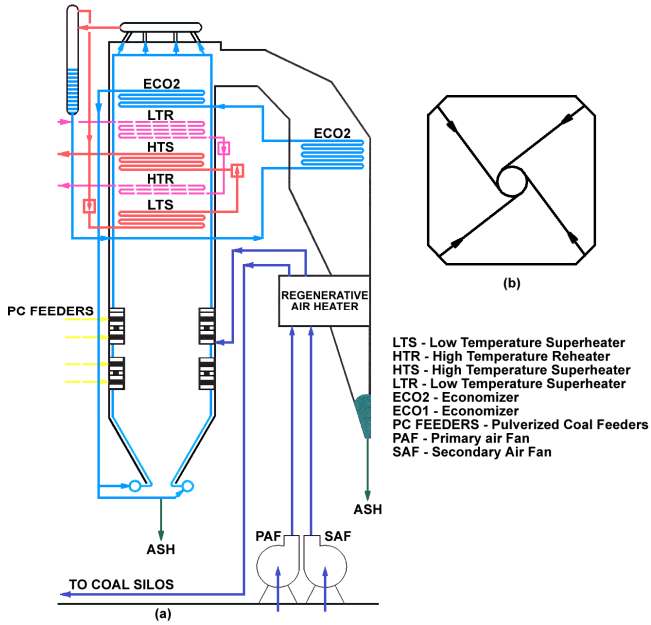

Figure 2 - (a) General disposition of the boiler components; (b) Horizontal cross section.

4. MESH SETTINGS AND CONVERGENCE CRITERIA

The domain under consideration comprises the first stage of the boiler: the combustion chamber with the burners at the corners and the heat exchangers until the top. The entrance to the second stage was considered the outlet of the domain. The discretization was done using tetrahedric volumes. As the boiler height corresponds to only six equivalent diameters of the boiler, the boundary layer is not developed at the whole domain. Nevertheless, prismatic volumes were used at the walls in order to capture the boundary layer behavior. Due to computational limitations, the mesh size used has approximately 1.5×10^6 elements, using mesh refinements in the chamber combustion. The convergence criterion adopted was the RMS – root mean square of the residual values, and the value adopted was 1×10^{-6} for all equations.

5. BOUNDARY CONDITIONS

The boundary conditions were obtained from the design data set and also from the daily operation data sheets. The operating conditions considered were the rated ones, for 160 MW. The following parameters were considered:

Inlet: The inlet conditions are those for air and coal flows entering the domain from the burner nozzles. Total primary and secondary combustion air and pulverized coal mass flow rates were set as 79.5 kg/s, 100 kg/s and 36 kg/s respectively. Temperatures of primary air and coal, and secondary combustion air were set as 542 K and 600 K respectively. Pulverized coal size was modeled by a probabilistic distribution and limited between 50 μm and 200 μm.

Outlet: The outlet boundary is the flue gas passage at lateral wall near the top of the boiler, just above the ECO 2 heat exchanger, where the mean static pressure was set.

Boiler walls: The boiler walls are covered with slanting tubes from the bottom until the beginning of the heat exchangers region; from there to the top the tubes are vertically positioned. Wall roughness, outlet temperature and thermal radiation coefficients were set for that two wall regions.

6. RESULTS

The simulation results were analyzed and compared with known data of the boiler operation. The main validation parameters were the temperature and mass fraction of some chemical species at the boiler outlet where regular measurements are made. As mentioned, two cases were compared, the horizontal and tilted burner jets. Figures 3 to 6 show the mass concentrations of methane, carbon monoxide, oxygen, NO_x and also temperature for two diagonal horizontal lines related to first and fourth burner levels.

The jet tilt reduces the concentration of CH_4 and CO on the analyzed regions (see Fig. 3). This can be due to the displacement of the flame and the resulting changes at the gas flow and particulate dynamics inside the boiler.

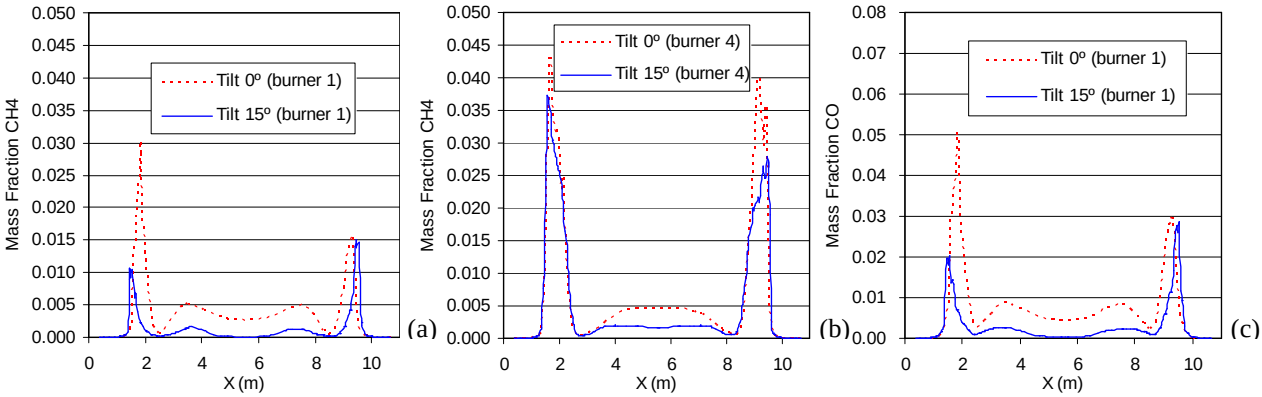

Figure 3 – Methane mass fractions on the burner lines 1 (a) and 4 (b), and CO mass fraction on the burner line 1 (c).

The NO_x concentrations presented at Fig. 4 follows an opposite trend, with the tilt of the burners enhancing the presence of the pollutant. For the first burner level the oxygen concentrations are also greater for the tilted burners than for the horizontal ones, as is shown at Fig. 5. This fact, associated to nitrogen availability and higher temperatures (see Fig. 6) creates the optimal conditions for NO_x formation.

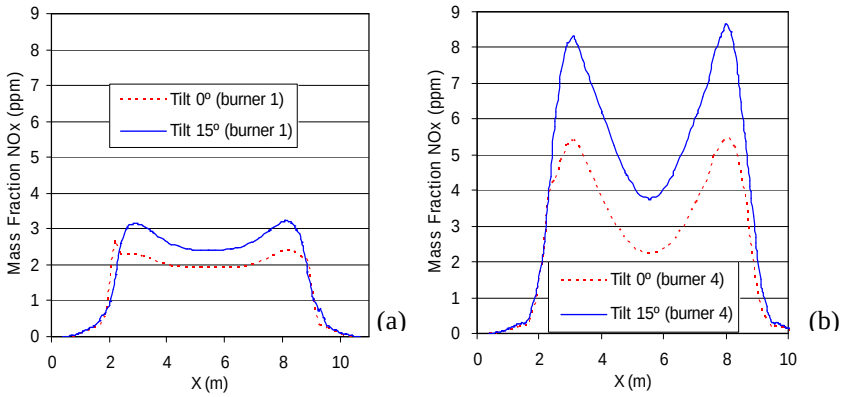

Figure 4 - NO_x mass fractions on the burner lines 1 (a) and 4 (b).

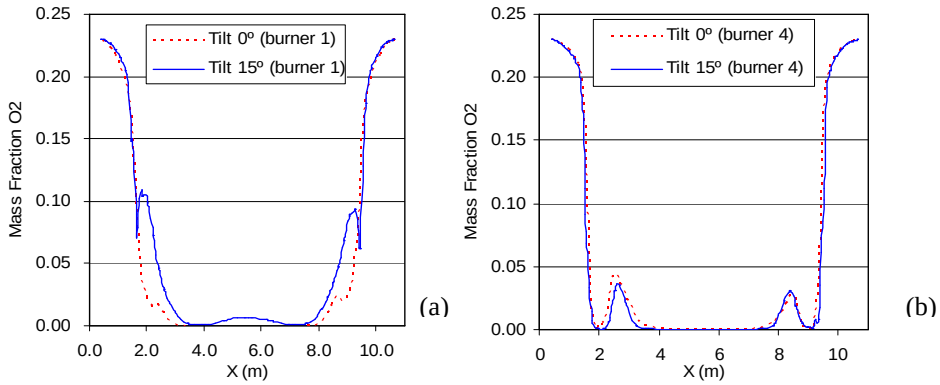

Figure 5 - Oxygen mass fractions on the burner lines 1 (a) and 4 (b).

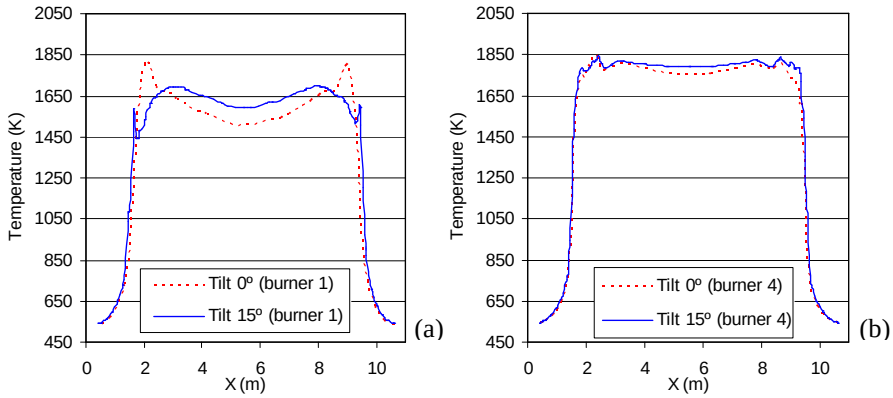

Figure 6 – Temperature distribution on the burner lines 1 (a) and 4 (b).

The increase of NO_x concentration on the fourth level of burners, shown at Fig. 4, is not due to the increase of oxygen concentration (see Fig. 5) at this region but instead to the sum of the contributions of the lower levels. Indeed, as there is a large concentration of volatiles at this region, most oxygen is consumed at the volatile and char oxidation reactions. The temperature and NO_x mass concentration at the vertical axis of the boiler is shown at Fig. 7. The temperature is a bit higher at lower positions in the boiler, due to the 15° upside down displacement of the fuel and air jets toward the boiler bottom level. The resulting lengthening of the residence time of the fuel particles at the chamber enhances the combustion process at these levels and also the heat flux at the walls, resulting in a similar temperature profile at boiler upper levels for both situations analyzed. Figure 7-b shows an increase of NO_x concentrations at the boiler center line, related to the air and fuel jets tilt, as explained above.

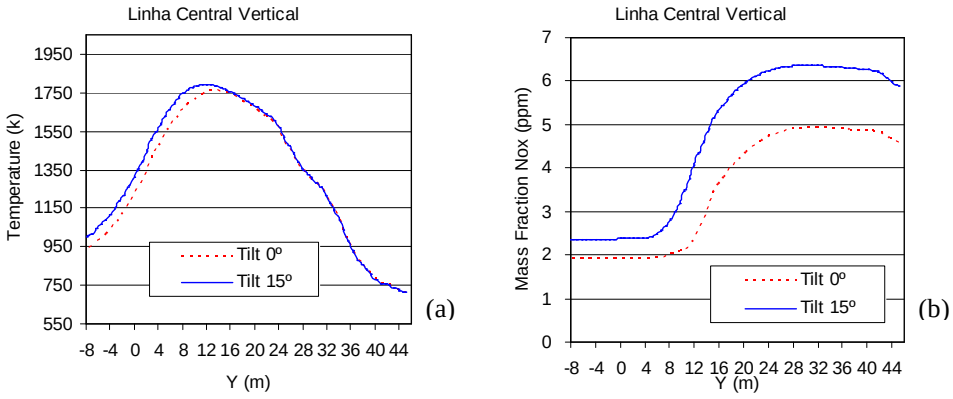

Figure 7 – Boiler central line: (a) Temperature distribution; (b) NO_x mass fractions.

Temperature and concentration data for the flue gases at the boiler outlet are presented at Tab. 1. The reduction of 13% in the oxygen quantity leaving the boiler is related to the enhancement of 21% in NO_x production at the combustion processes due to the burners tilt. The conclusion from the data analyses is that the advantage of burner tilt is only a more efficient burning process. There is a 70% reduction of carbon monoxide concentration at flue gases, due to the higher turbulence level and enlarged residence time, leading to a better mixing of air and fuel.

Table 1 – Global values at boiler flue gases outlet.

Flue gases outlet				
	Tilt 0º		**Tilt 15º**	
	Absolute value	**Relative**	**Absolute value**	**Relative**
Temperature ºC	455		449	
CO (kg/s)	0.074	377 ppm	0.022	111 ppm
CO2 (kg/s)	43.58	22.2%	44.59	22.7%
H2O (kg/s)	10.65	5.4%	10.71	5.4%
N2 (kg/s)	136.41	69.5%	136.41	69.4%
NO_x (kg/s)	0.00091	4.6 ppm	0.00110	5.6 ppm
O2 (kg/s)	5.71	2.9%	4.96	2.5%
Total flow (kg/s)	196.36		196.66	
Heat Flux at the Boiler Walls (W/m2)	103,711		107,326	

The standard data of the boiler design were used at the present study. Only the burner tilts were changed. The flue gases mass fractions should be taken in qualitative sense, only their relative values for the situations under comparison are of significance. Indeed, their absolute values did not agree with the actual values during the boiler operation because, at the last years, some alterations were made on the boiler, as at the physical structure as at the operation processes.

7. CONCLUSIONS

In the present work the commercial software CFX has been used to study the influence of heterogeneous inlet flow of fuel and air on the NO_x formation in a boiler of a 160 MW thermal power plant. Two different operation situations were analyzed, one with horizontal jets of fuel and air; the other with a -15º displacement (upside-down jets) on the injection of fuel and air relative to the horizontal plane. It was verified that this little change on the operation process resulted in significant alterations on the behavior of the combustion process. This change, introducing a -15º displacement on the injection of fuel and air relative to the horizontal plane, was made in order to improve the combustion efficiency, as confirmed by the simulation results, and to assist the maintenance of the combustion process. However, this alteration causes, in this case, a significant increase on the NO_x emissions. The main goal of this work is to show the importance of numerical simulations on actual processes in actual plants. The results can help to verify if an alteration on a particular parameter would really improve the process or not, and if it would result in other collateral effects or not.

8. REFERENCES

Abbas, T., Costen, P., Lockwood, F. C. and Romo-Millares, C. A., 1993, "The Effect of Particle Size on NO Formation in a Large-Scale Pulverized Coal-Fired Laboratory Furnace: Measurements and Modeling", Combustion and Flame, v. 93, pp. 316-326.

Backreedy, R. I., Fletcher, L. M., Ma, L., Pourkashanian, M. and Williams, A., 2006, "Modelling Pulverised Coal Combustion Using a Detailed Coal Combustion Model", Combust. Sci. and Tech., 178: 763-787.

Bosoaga, A., Panoiu, N., Mihaescu, L., Backreedy, R. I., Ma, L., Pourkashanian, M. and Williams, A., 2006, "The combustion of pulverized low grade lignite", Fuel, v. 85, pp. 1591-1598.

Brown, W. K., 1995, "Derivation of the Weibull distribution based on physical principles and its connection to the Rosin-Rammler and lognormal distributions", Journal of Applied Physics, v. 78, n. 4, pp. 2758-2763.

Carvalho, M.G., Farias, T. and Fontes, P., 1991. "Predicting radiative heat transfer in absorbing, emitting, and scattering media using the discrete transfer method", ASME HTD, Vol. 160, pp.17-26.

CFX Solver Theory, 2004.

Eaton, A. M., Smoot, L. D., Hill, S. C. and Eatough, C. N., 1999, "Components, formulations, solutions, evaluations, and applications of comprehensive combustion models", V. 25, pp. 387-436.

Kanury, A. M., 1975, "Introduction to Combustion Phenomena", Gordon and Beach Science Publishers, New York.

Knudsen, J. G., 1958, "Fluid Dynamics and Heat Transfer", Mc Graw Hill.

Launder, B.E. and Sharma, B.I., 1974. "Application of the energy-dissipation model of turbulence to the calculation of flow near a spinning disc", Letters in Heat and Mass Transfer, Vol. 19, pp. 519-524.

Kuo, K.K., 1996. "Principles of combustion", John Wiley & Sons, New York.

Kurose, R., Makino, H. and Suzuki, A., 2004, "Numerical analysis of pulverized coal combustion characteristics using advanced low-NO_x burner", v. 83, pp. 693-703.

Li, Z. Q., Wei, Y. and Jin, Y., 2003, "Numerical simulation of pulverized coal combustion and NO formation, Chemical Engineering Science", v. 58, pp. 5161-5171.

Magnussen B.F. and Hjertager B. H., 1976. "On mathematical models of turbulent combustion with special emphasis on soot formation and combustion". Proc. of the 16th Int. Symp. on Comb., The Combustion Institute, pp. 719–729.

Turns, S. T., 2000, "An introduction to combustion – Concepts and applications", 2nd, edn, McGraw-Hill, New York.

Ubhayakar, S. W., Stickler, D. B., Rosenberg Jr., C. W. and Gannon, R. E., 1976, "Rapid Devolatilization of Pulverized Coal in Hot Combustion Gases", Proceedings of the Combustion Institute, pp. 427-436.

Williams, A., Pourkashanian, M., Jones, J. M. and Skorupska, N., 2000, "Combustion and Gasification of Coal", Taylor & Francis, New York.

Xu, M., Azevedo, J. L. T. and Carvalho, M. G. , 2000, "Modelling of the combustion process and NO_x emission in a utility boiler", Fuel, vol. 79, pp. 1611-1619.

Zhang, Y., Wei, X., Zhou, L. and Sheng, H., 2005, "Simulation of coal combustion by AUSM turbulence-chemistry char combustion model and a full two-fluid model", v. 84, pp. 1798-1804.

9. RESPONSIBILITY NOTICE

The authors are the only responsible for the printed material included in this paper.